



# Pressure-Assisted Sinter-Bonding Characteristics at 250 °C in Air Using Bimodal Ag-Coated Cu Particles

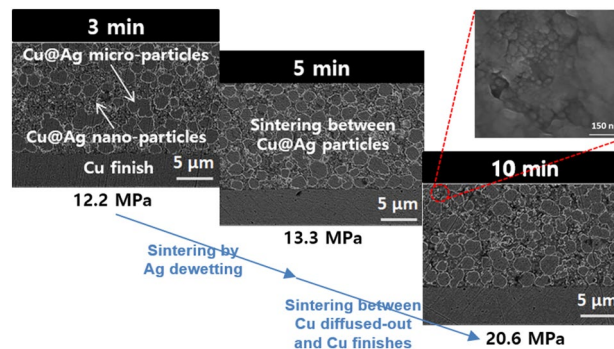
Sung Yoon Kim<sup>1</sup> · Myeong In Kim<sup>1</sup> · Jong-Hyun Lee<sup>1</sup>

Received: 10 December 2019 / Accepted: 20 February 2020 / Published online: 2 April 2020  
© The Korean Institute of Metals and Materials 2020

## Abstract

To achieve bondlines with improved heat resistance and thermal conductance during operation, pressure-assisted sinter-bonding was performed in air with bimodal Ag-coated Cu particles for die attachment of the next-generation power devices composed of SiC. The bonding temperature and pressure were 250 °C and 10 MPa, respectively, and the sizes of the bimodal particles were 2 μm and 350 nm. After a short bonding time of 10 min, a paste with a 6:4 mixing ratio showed an average shear strength of > 20 MPa. The dewetting of Ag shells on the particles and void filling by the 350 nm particles induced rapid sintering.

## Graphic Abstract



**Keywords** Sinter-bonding · Ag-coated · Cu particle · Bimodal particle · Ag dewetting · Shear strength

## 1 Introduction

Soldering technology significantly impacts the electrical and electronic industries, and has been widely used as the main method for the interconnection and mounting of various electronic devices since the late 1990s [1, 2]. Soldering, which can rapidly connect many components, has a reliability problem, and suffers from remelting and drastic deterioration in mechanical properties when applied

for high-heat-generating devices due to the inherently low melting points of solders [3, 4]. Therefore, for the relatively high operating temperatures of wide-band-gap (WBG) semiconductors such as SiC, Pb-bearing solders with Ag have been applied. Ag can be sinter-bonded at significantly lower temperatures than its melting point, and the bondline formed exhibits high heat endurance and heat conductance [5–7]. However, issues such as Ag migration and material cost have necessitated the development of low-cost Cu-based materials with thermal and electrical conductivities similar to those of Ag [8–10]. Therefore, an important topic in die attachment using Cu is the reduction of the sintering temperature and time.

✉ Jong-Hyun Lee  
pljh@snut.ac.kr

<sup>1</sup> Department of Materials Science and Engineering, Seoul National University of Science and Technology, 232 Gongneung-ro, Nowon-gu, Seoul 01811, Republic of Korea

Sinter-bonding studies using Cu particles have been performed under a reducing or inert atmosphere [5], and these studies have also shown that pastes containing Cu particles exhibit the best compatibility with Cu finishes [11]. In addition, the use of minute Cu particles in the paste is favorable for high-speed sinter-bonding [11, 12]. Nevertheless, the full adoption of minute particles is counterproductive because of the drawbacks concerning mixing and material costs.

Herein, high-speed die sinter-bonding on Cu-finish interfaces at a relatively low temperature of 250 °C in air was performed using a low-cost Ag-coated Cu (Cu@Ag) particle-based paste. Sinter-bonding was possible with external pressure because the Ag shell on the Cu@Ag particle effectively suppressed the surface oxidation of the core Cu particle [13, 14]. To achieve fast sinter-bonding at 10 MPa, bimodal pastes containing 2  $\mu\text{m}$  and 350 nm Cu@Ag particles were investigated.

## 2 Experimental

Small Cu particles of 350 nm were wet synthesized in-house [15] and large Cu particles (average size: 2  $\mu\text{m}$ , Join M, Republic of Korea) were purchased. The small and large Cu

particles were coated with approximately 20 wt% Ag shells via electroless plating using a previously reported method [16]. Thus, small and large Cu@Ag particles were obtained. Further, the small and large Cu@Ag particles were mixed in ethanol at a specific mixing ratio using ultrasonic treatment for 10 min, the slurry mixture was dried in vacuum chamber. Subsequently, the resulting mixture of small and large Cu@Ag particles was mixed with a prepared reducing solvent using a spatula to obtain the pastes. The particle-to-solvent weight ratio was determined to be 82:18.

Die attachment was performed by sinter-bonding a dummy Cu die on a dummy Cu substrate. The areas of the dummy Cu die and dummy Cu substrate were 3  $\times$  3 mm<sup>2</sup> and 10  $\times$  10 mm<sup>2</sup>, respectively. Firstly, the prepared Cu@Ag particle-based paste was preferentially stencil-printed onto the substrate through a mask with a slit of 3  $\times$  3  $\times$  0.1 mm<sup>3</sup>. Subsequently, the die was aligned and placed on the printed pattern and the sandwich-structured sample was heated at 250 °C. Sinter-bonding was performed in air at 10 MPa throughout the bonding. The bonding was conducted up to 10 min.

The initial morphologies and cross-sectional microstructures of the prepared Cu@Ag particles, the microstructures of bondlines after bonding, and fracture surfaces after shear tests were examined using a high-resolution scanning

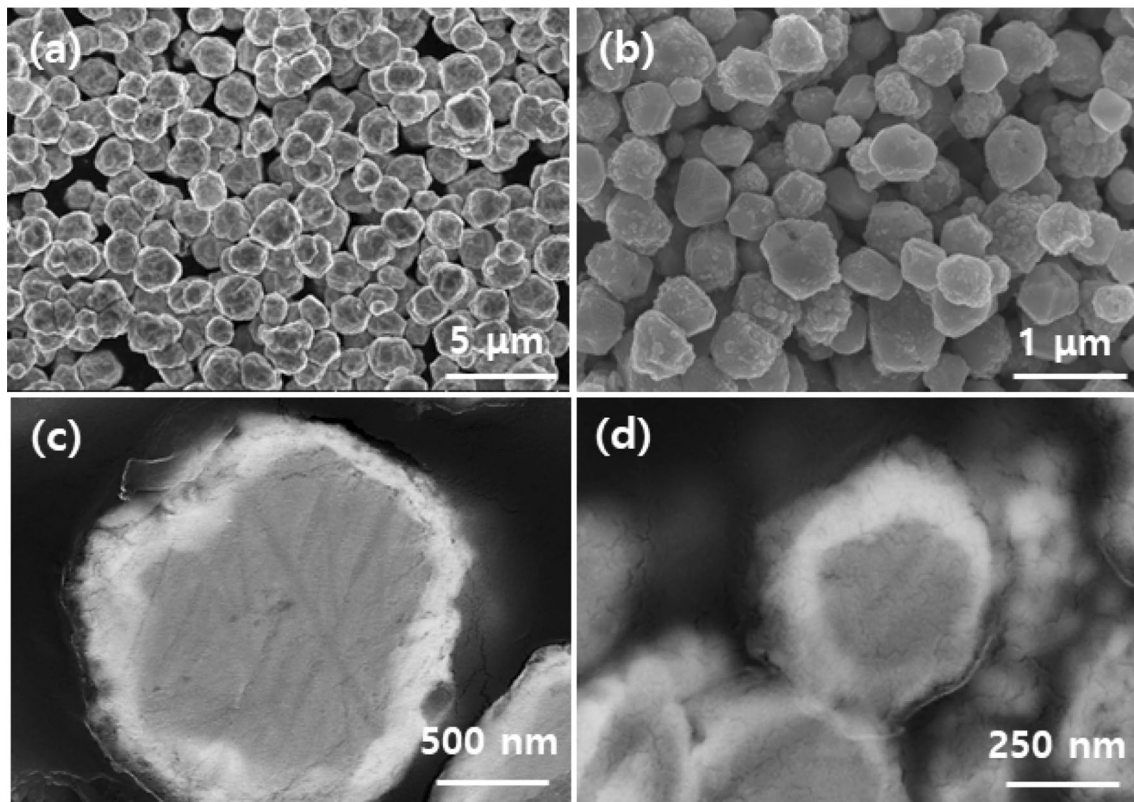


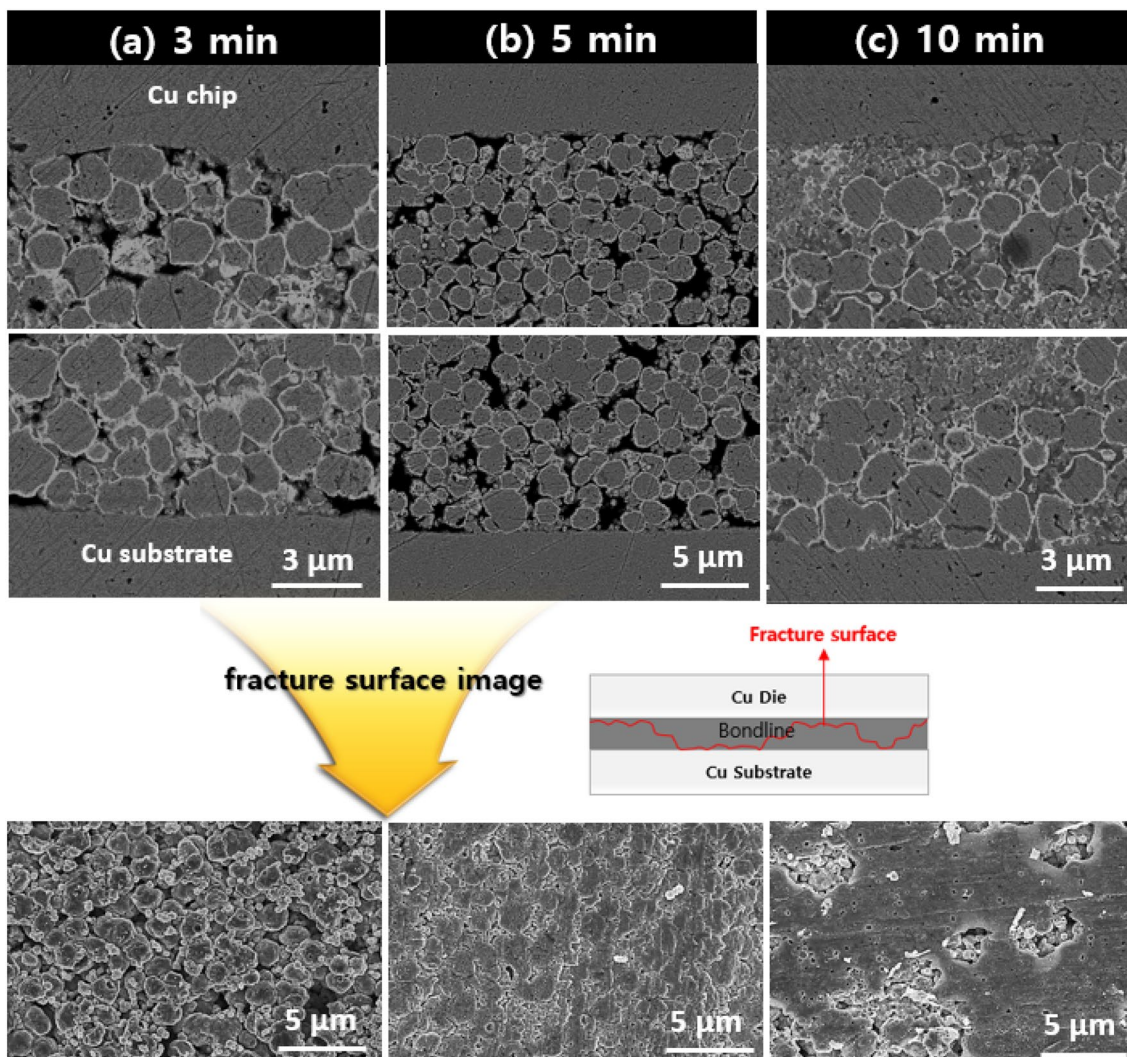
**Fig. 1** a, b SEM and c, d cross-sectional back-scattered electron images of the a, c 2  $\mu\text{m}$  and b, d 350 nm Cu@Ag particles

electron microscope (HR-SEM; SU8010, Hitachi). The bonding strength of the bondline was measured using a bond tester (Dage 4000, Nordson DAGE) and defined as the maximum stress value measured during shearing at 200  $\mu\text{m/s}$  at a height of 200  $\mu\text{m}$  from the substrate surface.

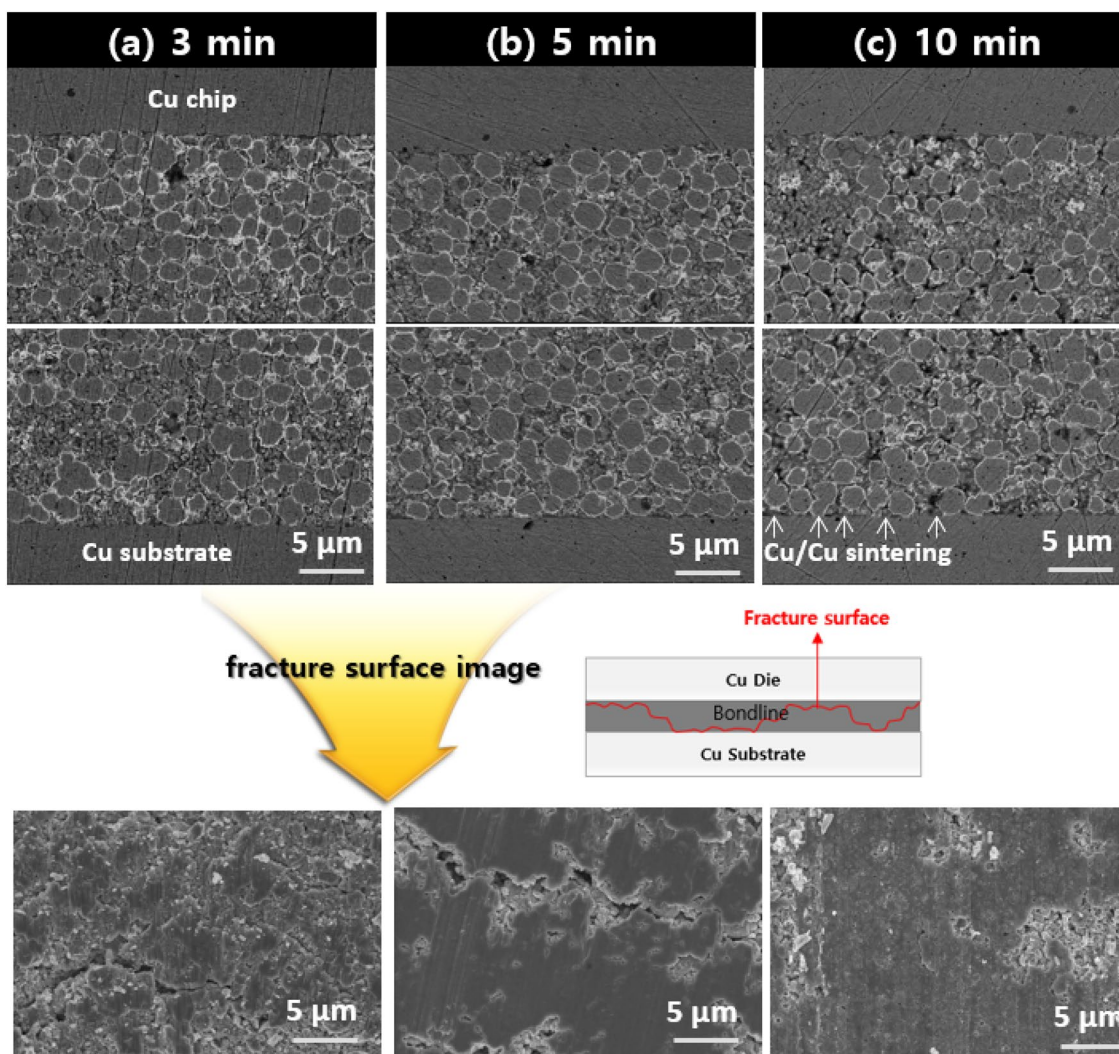
### 3 Results and Discussion

Figure 1a, c show the appearance and internal images of the 2  $\mu\text{m}$  Cu@Ag particles. The surfaces were rough and the average thickness of the Ag coating was calculated to be approximately 55 nm. The initial images of the 350 nm Cu@Ag particles are shown in Fig. 1b, d. The average thickness of the Ag coating in the 350 nm Cu@Ag particles significantly decreased to approximately 10 nm due to the drastic increase in the total surface area.

The bondline microstructure as a function of bonding time was examined after mixing the large and small Cu@Ag particles in an 8:2 ratio, and is presented in Fig. 2a–c. The cross-section sintered for 3 min showed localized sintering at contacts between the Ag shells dewetted from the particles, but large voids were frequently observed due to the shortage of 350 nm particles and short bonding time. Although the voids were still present with increasing bonding time to 5 min, they were eliminated when the bonding time was 10 min. Consequently, the densities of the bondlines notably increased with increasing bonding time due to the enhanced sintering degree, and the trend was similar in the fracture surfaces. However, all fractures occurred both at the chip/bondline and bondline/substrate interfaces across the bondline, indicating that the weakest bonding was present at the interfaces.



**Fig. 2** Cross-sectional BSE images of the bondlines sintered at a mixing ratio of 8:2 and fracture surfaces on dies with various bonding times: **a** 3, **b** 5, and **c** 10 min



**Fig. 3** Cross-sectional BSE images of the bondlines sintered at a mixing ratio of 6:4 and fracture surfaces on dies with various bonding times: **a** 3, **b** 5, and **c** 10 min

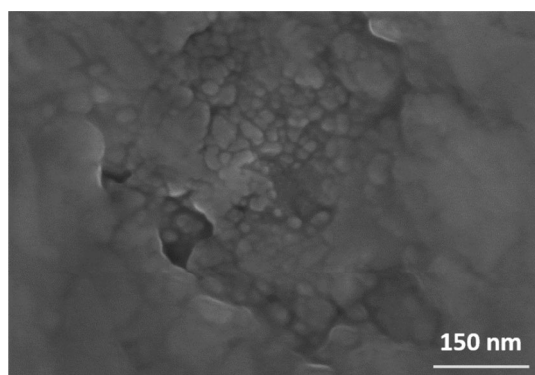


**Fig. 4** Magnified image of the cross-sectional bondline shown in Fig. 3c, showing the dewetted Ag nodules

Figure 3 shows the microstructures and fracture surfaces of the bondlines sinter-bonded using a paste prepared by mixing the large and small Cu@Ag particles in a 6:4 ratio. When the amount of 350 nm particles was increased, the density of the bondline microstructure was significantly increased only after 3 min of sintering. When the bonding time was increased from 3 to 10 min, the fracture surface density also proportionally increased. However, the difference in the low-magnification bondline images was not significant. Therefore, when the 350 nm particles were present in sufficient amounts, sintering between the particles was significantly enhanced. Nevertheless, fracture surfaces still formed at the chip/bondline and bondline/substrate interfaces.

When the Cu@Ag particles were heated to 250 °C, the interfacial instability caused by the significant lattice mismatch of Ag and Cu caused the Ag shells of all the particles

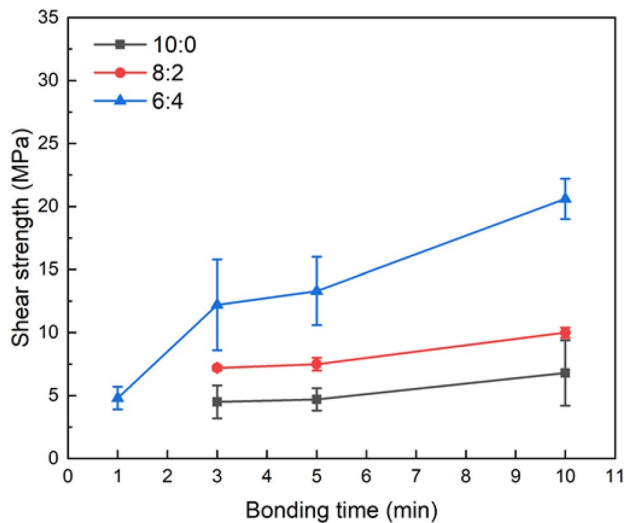


**Fig. 5** Shear strength of the Cu dummy dies sinter-bonded at 250 °C in air at 10 MPa with various mixing ratios and bonding times

to be dewetted on the surfaces of Cu, as shown in Fig. 4, depending on the particle size [17–19]. Thus, the Ag shells on the 350 nm particles dewetted at lower temperatures and temporarily behaved like a quasi-fluid owing to the Gibbs-Thompson effect at the thickness of 10 nm [5, 14]. Eventually, the dewetted Ag exhibited flowability to decrease and eliminate the voids inside the bondline in the well-contacted environment between the particles due to the initial high-packing density and pressure as well as the excellent sinterability of the Ag nano-nodules dewetted on the 2 μm particles. In addition, the reducing solvent used herein can remove the oxide layer on the Cu finish and permit sinter-bonding on the Cu finish. Consequently, additional sinter-bonding between the Cu diffused-out through the locally thin Ag layers from the core and the Cu finish was also observed (Fig. 3c) [20]. However, fracturing at the chip/bondline and bondline/substrate interfaces implied that the sinter-bonding at the interfaces remained weak.

Figure 5 shows the shear strength of the Cu dummy dies with respect to the mixing ratios and bonding time. Bonding using the single-modal Cu@Ag particle (10:0) resulted in the lowest shear strength after 10 min of bonding, despite the increase in shear strength values with increasing bonding time. When a bimodal mixing ratio of 8:2 was applied, the shear strength generally increased at all studied bonding times, but the values remained relatively low. Meanwhile, the shear strength values obtained using the bimodal particles mixed in the 6:4 ratio were significantly enhanced, and the increasing trend with the bonding time accelerated. The increased amount of the 350 nm particles can facilitate more robust adhesions at the particle/Cu finish interfaces by increasing the contact areas. Furthermore, relatively long bonding times can change the sinter-bonding between

dewetted Ag and Cu finishes into the sinter-bonding with improved matching between the Cu diffused-out through the Ag layers and Cu finishes, thus improving the bonding strength. As a representative result, a sufficient shear strength of > 20 MPa was obtained at a short sinter-bonding time of 10 min, which indicates higher bondability than a case of the sinter-bonding at identical temperature in forming gas using Cu nanoaggregates [21]. This strength is similar to that of the die attached using conventional Pb-5Sn solders [17], with shorter bonding times than those previously reported when micrometer-sized Ag particles were used under reducing or inert conditions [5].

## 4 Conclusions

When a bimodal paste containing 2 μm and 350 nm Cu@Ag particles mixed in a ratio of 6:4 was used, a sufficient shear strength of > 20 MPa was obtained after a short bonding time of 10 min at 250 °C and 10 MPa. The rapid sinter-bonding was attributed to the dewetting phenomenon of the Ag shells, especially in the 350 nm particles. However, fracturing at the bondline/Cu finish interfaces indicated that the sinter-bonding between the dewetted Ag and Cu finishes remained weak. This facile sinter-bonding at low temperatures in air is a competitive method for the attachment of WBG power devices.

**Acknowledgements** This research was supported by the Commercialization Promotion Agency for R&D Outcomes (COMPACT) funded by the Ministry of Science and ICT (MSIT) [Optimization of fabrication processes for the mass production of Ag-coated Cu powder of average size 1.4 μm and 400 nm and evaluation of the application properties].

## References

- Kim, J., Park, C., Cho, K.-M., Hong, W., Bang, J.-H., Ko, Y.-H., Kang, N.: Oxidation and repeated-bending properties of Sn-based solder joints after Highly Accelerated Stress Testing (HAST). *Electron. Mater. Lett.* **14**, 678–688 (2018)
- Cho, S., Ko, Y.: Finite element analysis for reliability of solder joints materials in the embedded package. *Electron. Mater. Lett.* **15**, 287–296 (2019)
- Wang, T., Chen, X., Lu, G.Q., Lei, G.Y.: Low-temperature sintering with nano-silver paste in die attached interconnection. *J. Electron. Mater.* **36**, 1333–1340 (2007)
- Siow, K.S., Lin, Y.T.: Identifying the development state of sintered silver (Ag) as a bonding material in the microelectronic packaging via a patent landscape study. *J. Electron. Packag.* **138**, 020804 (2016)
- E. Ide, S. Angata, A. Hirose, K.F. Kobayashi: Metal–metal bonding process using Ag metallo-organic nanoparticles. *Acta Mater.* **53**, 2385–2393 (2005)
- Noh, S., Choe, C., Chen, C., Zhang, H., Sukanuma, K.: Printed wire interconnection using Ag sinter paste for wide band gap

- power semiconductors. *J. Mater. Sci. Mater. Electron.* **29**, 15223–15232 (2018)
7. Chang, T.C., Lee, C.C., Hsieh, C.P., Hung, S.C., Cheng, R.S.: Electrical characteristics and reliability performance of IGBT power device packaging by chip embedding technology. *Microelectron. Reliab.* **55**, 2582–2588 (2015)
  8. S. Krishnan, A. Haseeb, M.R. Johan: Preparation and low-temperature sintering of Cu nanoparticles for high-power devices. *IEEE Trans. Compon. Packag. Manuf. Technol.* **2**, 587–592 (2012)
  9. Morisada, Y., Nagaoka, T., Fukusumi, M., Kashiwagi, Y., Yamamoto, M., Nakamoto, M.: A low-temperature bonding process using mixed Cu–Ag nanoparticles. *J. Electron. Mater.* **39**, 1283–1288 (2010)
  10. Noh, B.I., Yoon, J.W., Kim, K.S., Kang, S., Jung, S.B.: Electrochemical migration of directly printed Ag electrodes using Ag paste with epoxy binder. *Microelectron. Eng.* **103**, 1–6 (2013)
  11. Lu, G.Q., Wang, M., Mei, Y., Li, X.: Advanced die-attach by metal-powder sintering: the science and practice. In: *Proceedings of 10th International Conference on Integrated Power Electronic System: (CIPS 2018)*, pp. 594–602 (2018)
  12. Jianfeng, Y., Guisheng, Z., Anming, H., Zhou, Y.N.: Preparation of PVP coated Cu NPs and the application for low-temperature bonding. *J. Mater. Chem.* **40**, 15981–15986 (2011)
  13. Lee, C.H., Choi, E.B., Lee, J.-H.: Characterization of novel high-speed die attachment method at 225 C using submicrometer Ag-coated Cu particles. *Scr. Mater.* **150**, 7–12 (2018)
  14. Chee, S.S., Lee, J.-H.: Preparation and oxidation behavior of Ag-coated Cu nanoparticles less than 20 nm in size. *J. Mater. Chem. C* **2**, 5372–5381 (2014)
  15. Choi, E.B., Lee, J.-H.: Preparation of submicroscale Ag-coated Cu particles by multi-step addition of Ag plating solution and antioxidation properties for different Ag shell thicknesses. *Arch. Metall. Mater.* **62**, 1137–1142 (2017)
  16. Choi, E.B., Lee, J.-H.: Submicron Ag-coated Cu particles and characterization methods to evaluate their quality. *J. Alloys Compd.* **689**, 952–958 (2016)
  17. X. Yu, J. Li, T. Shi, C. Cheng, G. Liao, J. Fan, Z. Tang: A green approach of synthesizing of Cu–Ag core-shell nanoparticles and their sintering behavior for printed electronics. *J. Alloys Compd.* **724**, 365–372 (2017)
  18. P.A. Huttunen, J. Mäkinen, A. Vehanen: Defects in heteroepitaxial structures studied with monoenergetic positrons: large-lattice-mismatch systems Cu/Ag (111) and Ag/Cu (111). *Phys. Rev. B* **41**, 8062–8074 (1990)
  19. Muzikansky, A., Nanikashvili, P., Grinblat, J., Zitoun, D.: Ag dewetting in Cu@Ag monodisperse core-shell nanoparticles. *J. Phys. Chem. C* **117**, 3093–3100 (2013)
  20. Liu, X., Nishikawa, H.: Low-pressure Cu–Cu bonding using in-situ surface-modified microscale Cu particles for power device packaging. *Scr. Mater.* **120**, 80–84 (2016)
  21. J. Li, Q. Liang, T. Shi, J. Fan, B. Gong, C. Feng, J. Fan, G. Liao, Z. Tang: Design of Cu nanoaggregates composed of ultra-small Cu nanoparticles for Cu–Cu thermocompression bonding. *J. Alloys Compd.* **772**, 793–800 (2019)

**Publisher's Note** Springer Nature remains neutral with regard to jurisdictional claims in published maps and institutional affiliations.